

Dielectric, piezoelectric properties and temperature stability in modified (Na,K,Li)(Nb,Ta)O₃ ceramics for piezoelectric energy harvesting device

Sunmin Byeon · Juhyun Yoo

Received: 28 March 2013 / Accepted: 30 May 2014 / Published online: 10 June 2014
© Springer Science+Business Media New York 2014

Abstract In this study, modified (Na,K,Li)(Nb,Ta)O₃((Na_xK_{1-x})_{0.96}Li_{0.04}(Nb_{0.90}Ta_{0.10})_{0.998}Zn_{0.005}O₃) ceramics were fabricated using a normal sintering technique. The dielectric and piezoelectric properties of the resulting ceramics were studied with special emphasis on the varying sodium concentration. The results of X-ray diffraction patterns show that the specimen exhibits an orthorhombic perovskite phase structure. High physical properties of $d_{33}=261$ pC/N, $k_p=0.44$, $\epsilon_r=735$, $\rho=4.53$ g/cm³ and $d_{33}\cdot g_{33}=10.47$ pm²/N were obtained from the composition ceramics with $x=0.56$ at room temperature. $\Delta k_p/k_{p20^\circ\text{C}}$ and $\Delta f_r/f_{20^\circ\text{C}}$ showed the maximum value of 0.034 and -0.025 at 40 °C and 50 °C, respectively. Also, the temperature stability of d_{33} , g_{33} and $d_{33}\cdot g_{33}$ of specimen with $x=0.56$ was an excellent. Therefore, it is considered that the temperature stability of electrical properties is suitable for the applications of piezoelectric actuator, sensor and energy harvester.

Keywords Temperature stability · Electromechanical coupling coefficient (k_p) · Piezoelectric charge constant (d_{33}) · Piezoelectric voltage constant (g_{33})

1 Introduction

Lead-based piezoelectric ceramics such as Pb (Zr,Ti)O₃ (abbreviated as PZT) have been widely used as piezoelectric energy harvesters and piezoelectric actuators because of their excellent piezoelectric properties [1, 2]. However, the lead-based piezoelectric ceramics

containing PbO >60 wt% can cause serious environmental pollution and human health problems because of its high toxicity. Therefore, many studies for environment friendly Pb-free piezoelectric materials have been widely performed [3, 4].

(Na_{0.5}K_{0.5})NbO₃ (abbreviated as NKN) ceramics generally show low piezoelectric properties via the high volatilization of potassium and sodium during sintering process. The piezoelectric properties of the ceramics can be improved through the formation of solid solutions with other ABO₃-type ferroelectrics or non-ferroelectrics [5, 6]. In addition, an improvement in the microstructure of NKN-based piezoelectric ceramics was reported by the addition of novel sintering aids such as K_{5.4}C_{1.3}T₁₀O₂₉, CuO, ZnO [7–12] or ternary component substitutions such as BaTiO₃ [13], SrTiO₃ [14], CaTiO₃ [15]. However, these systems have the high performance sensitivity for stoichiometry and sintering temperature, poor durability against water, and low stability of piezoelectric properties, etc. In order to solve the above problems, various techniques, such as spark plasma sintering, hot isostatic pressing as well as sintering using double crucibles have been applied [16].

The enhancement of piezoelectric properties of the modified NKN-based ceramics is generally attributed to the polymorphic phase transition (PPT) temperature near or at room temperature. However, the strongly temperature-dependent behaviors of the piezoelectric properties near the PPT of these ceramics were not suitable for practical device applications. Therefore, the key approach for enhancing the temperature stability and avoiding the degradation of piezoelectric properties is to shift the PPT temperature (orthorhombic–tetragonal phase transition [T_{o-t}]) above room temperature. In general, generating energy of piezoelectric energy harvesting device is proportional to the value of $d_{ij}\cdot g_{ij}$ [12, 17–21].

S. Byeon · J. Yoo (✉)
Department of Electrical Engineering, Semyung University, Jechon,
Chungbuk 390-711, South Korea
e-mail: juhyun57@semyung.ac.kr

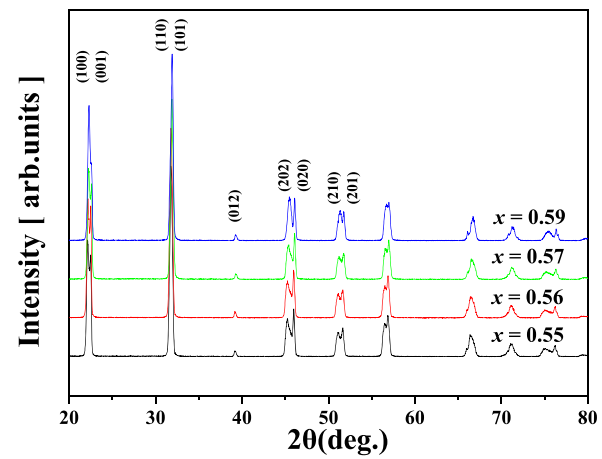
In this work, in order to develop lead free piezoelectric ceramics for the application of energy harvesting device with higher d_{33} · g_{33} and good temperature stability, the $((\text{Na}_x\text{K}_{1-x})_{0.96}\text{Li}_{0.04}(\text{Nb}_{0.90}\text{Ta}_{0.10})_{0.998}\text{Zn}_{0.005}\text{O}_3)$ (abbreviated as $\text{N}_x\text{K}_{1-x}\text{LNTZ}$ ($x=0.55\sim 0.59$) ceramics substituted with Zn were accurately selected and prepared using a conventional sintering method. We studied the microstructure, T_{o-t} and T_c phase transition behavior, piezoelectric properties and temperature stability of the resulting ceramics.

2 Experimental

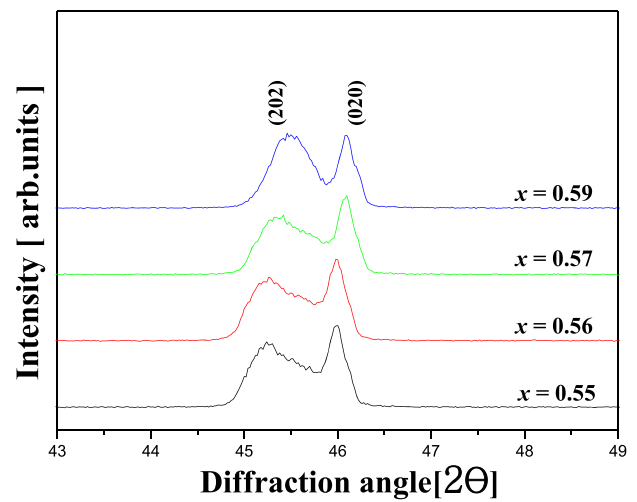
The raw materials such as Li_2CO_3 (Junsei), Na_2CO_3 (Junsei), K_2CO_3 (Junsei), Nb_2O_5 (Junsei), Ta_2O_5 (Kanto chemical) and ZnO (Junsei) with the purity above 99 % were used to prepare $\text{Li}_{0.04}(\text{Na}_x\text{K}_{1-x})_{0.96}(\text{Nb}_{0.90}\text{Ta}_{0.10})_{0.998}\text{Zn}_{0.005}\text{O}_3$ ($x=0.55\sim 0.59$) ceramics using a conventional mixed oxide method. The composition was weighted by mol ratio and the powders were ball-milled in plastic jar for 24 h (240 rpm) using acetone (Ball mill drive, NANOINTECH, Korea). After drying, they were calcined at 900 °C for 6 h. Thereafter, calcined powders were ball-milled and dried again. Polyvinyl alcohol (PVA) was added to the dried powders. The powders were molded by the uniaxial pressure of 22 MPa in a mold with a diameter of 21 mm (Ceramic press, AN JEON HYDRAULIC, Korea), burned out at 600 °C for 3 h, and then sintered at 1110 °C for 5 h. The specimens were polished into 1 mm thickness and then printed electrode at both side with silver paste by screen printing method. Poling was carried out at 120 °C in a silicon oil bath by applying fields of 40 kV/cm for 30 min.

The density of specimens was calculated using the Archimedes method. The microstructure of sintered surface was observed using scanning electron microscopy (SEM, S-2400, Hitachi, Japan) and grain size was measured using Linear intercept technical method. The crystal structure was determined using X-ray diffraction (XRD, X-ray Diffraction, D/MAX-2500H, Rigaku, Japan) with Cu $K\alpha$ radiation ($\lambda=1.5406 \text{ \AA}$). The dielectric properties were measured using an LCR meter (ANDO4034). The electromechanical coupling coefficient k_p was calculated using the resonance–anti resonance method with an impedance analyzer (Agilent 4294A; Agilent Technologies, USA) [22]. The piezoelectric constant d_{33} was measured using a piezo d_{33} meter (YE 2730A; APC, USA). The value of g_{33} constant was calculated using below equation;

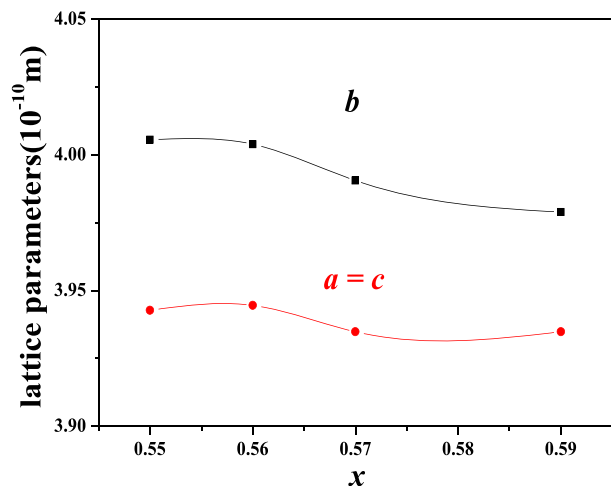
$$g_{33} = \frac{d_{33}}{\epsilon_{33}^T} [Vm/N]$$



(a)



(b)



(c)

Fig. 1 X-ray diffraction pattern of specimens as a function of sodium concentration

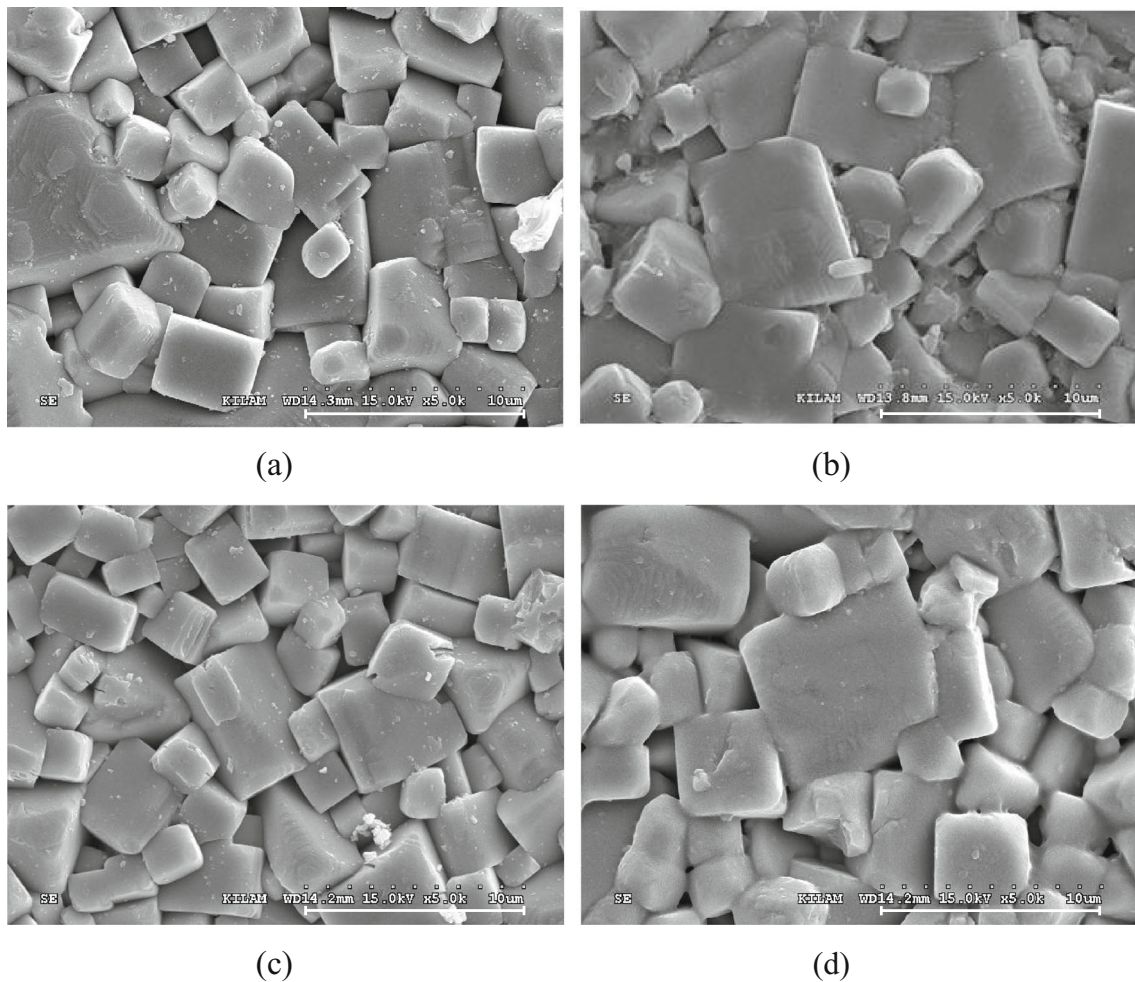


Fig. 2 Scanning electron microscopy microstructure of specimens as a function of sodium concentration

Temperature coefficients of k_p and resonance frequency (f_r) were calculated in the temperature range of -20 to 80 °C as shown in the following equations: [19].

$$\Delta k_p / k_p 20^\circ\text{C} = (k_p - k_p 20^\circ\text{C}) / k_p 20^\circ\text{C}$$

And

$$\Delta f_r / f_r 20^\circ\text{C} = (f_r - f_r 20^\circ\text{C}) / f_r 20^\circ\text{C}$$

3 Results and discussion

Figure 1(a) shows the XRD pattern of specimens as a function of sodium concentration. All the specimens showed a pure perovskite phase with an orthorhombic symmetry structure without a secondary phase. Figure 1(b) shows the magnified XRD pattern in the range of 2θ from 43 to 49° . The diffraction peaks (202) and (020) were slightly shifted to the higher angle and the orthorhombic peaks slightly increased with increasing

Table 1 Physical properties of specimens as a function of sodium concentration

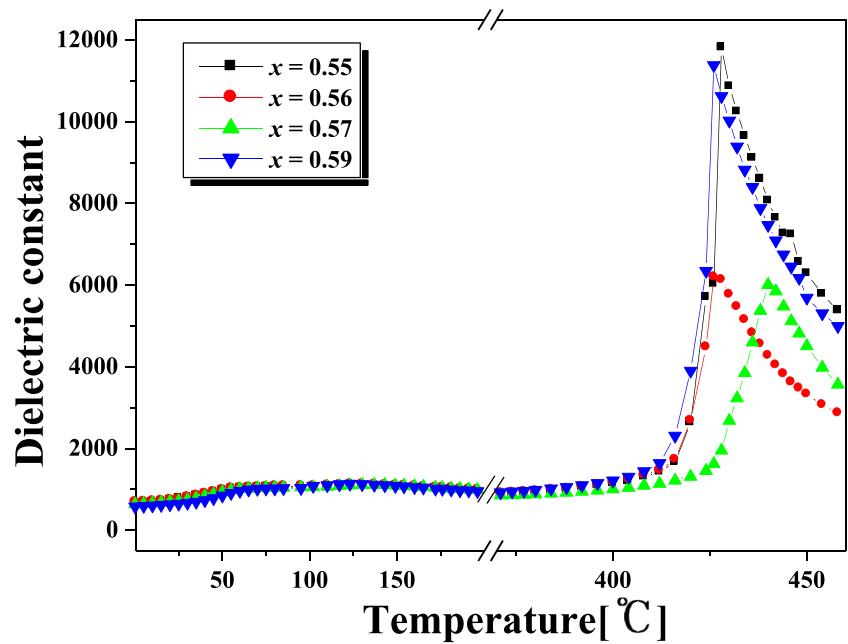
| x | Density (g/cm^3) | k_p | Q_m | d_{33} (pC/N) | ϵ_r | T_{o-t} ($^\circ\text{C}$) | T_c ($^\circ\text{C}$) | g_{33} (10^{-3} Vm/N) | $d_{33} \cdot g_{33}$ (pm^2/N) |
|------|------------------------------------|-------|-------|-----------------------------------|--------------|--------------------------------|----------------------------|---|--|
| 0.55 | 4.52 | 0.43 | 108.1 | 254 | 725 | 125 | 430 | 39.64 | 10.07 |
| 0.56 | 4.53 | 0.44 | 104.9 | 261 | 735 | 123 | 428 | 40.10 | 10.47 |
| 0.57 | 4.52 | 0.43 | 91.8 | 251 | 671 | 130 | 440 | 42.19 | 10.58 |
| 0.59 | 4.49 | 0.41 | 89.9 | 237 | 591 | 123 | 430 | 45.29 | 10.73 |

sodium concentration owing to a smaller ionic radius size of Na^+ (0.93 Å) than that of K^+ (1.33 Å) [23]. These Na substitution can increase the symmetry of a crystal probably by decrease in the length of a and c axes of an orthorhombic lattice ($a \approx c > b$ in a pure NKN). As shown in Fig. 1c, the lattice parameters of the perovskite primitive cell $a = c$ (Å), b (Å) and β (°) of 0.56 Na substituted specimen were observed as 3.944, 4.004 and 89.80, respectively. Since, $a = c$ (Å), b (Å) and β (°) of 0.59 Na substituted specimen were observed as

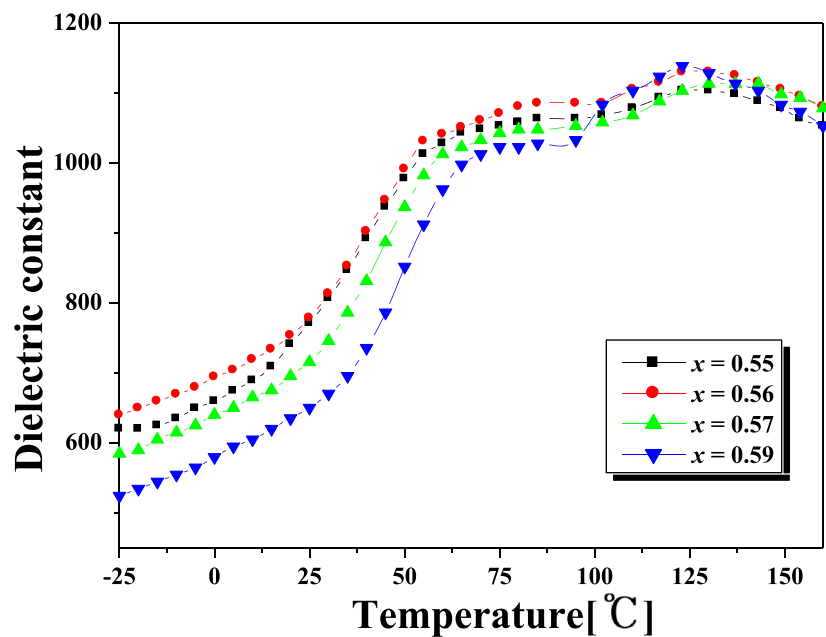
3.934, 3.987 and 90.00, respectively. As expected, the lattice parameters decreased with the increasing Na values. The result shows that the $a = c$ (Å) decreases and β (°) increases with increasing Na content. The relative density of the $\text{N}_x\text{K}_{1-x}\text{LNTZ}$ ceramics showed 96.4, 96.7, 95.4 and 95.5 % for the $x=0.55, 0.56, 0.57$ and 0.59 compositions, respectively.

Figure 2 shows SEM photographs of specimens as a function of sodium concentration. We took the SEM images from sintered surface. The SEM images showed the general

Fig. 3 Temperature dependence of dielectric constant of specimens as a function of sodium concentration



(a)



(b)

bimodal grain size distribution. The pores of the ceramics with $x=0.56$ exhibited a tendency to decrease. It is considered that the denser microstructure with lesser pores and grown grains may be due to the optimum sintering temperature of the ceramics. However, with further increasing sodium concentration, grain size of specimens was significantly decreased. It is also considered that these results are attributed to the degradation of sinterability of the ceramics according to the increase of sintering temperature due to the increase of NaNbO_3 (melting point = 1410 °C) composition ratio, compared with KNbO_3 (melting point = 1054 °C).

Table 1 shows the physical properties of specimens as a function of sodium concentration. The excellent physical properties of the piezoelectric constant (d_{33}) = 261 pC/N, electromechanical coupling factor (k_p) = 0.44, dielectric constant (ϵ_r) = 735, $d_{33} \cdot g_{33} = 10.47 \text{ pm}^2/\text{N}$, and density (ρ) = 4.53 g/cm³ were obtained from the composition ceramic with $x=0.56$. In this experiment, the poling of specimens was performed at 120 °C, which shows the coexistence of orthorhombic and tetragonal phase. Accordingly, higher d_{33} and k_p values appeared due to the increased polarization efficiency of the specimens [20]. In this experiment, when sodium increases to $x=0.59$, the piezoelectric voltage constant (g_{33}) reaches the remarkably highest values of $45.29 \times 10^{-3} \text{ Vm/N}$. The g_{33} value can increase relatively due to the decreased dielectric constants resulting from $g_{33} = d_{33}/\epsilon_{33}^T$. Moreover, while $d_{33} \cdot g_{33} = 10.466 \text{ pm}^2/\text{N}$ in the composition ceramic with $x=0.56$, the $d_{33} \cdot g_{33}$ in the composition ceramic with $x=0.59$ showed a higher value of $10.73 \text{ pm}^2/\text{N}$, compared with $9.293 \text{ pm}^2/\text{N}$ in PZT-5A and $3.141 \text{ pm}^2/\text{N}$ in Pb-free NKN ceramics [21]. However, this composition has a poor temperature stability of the dielectric constant (ϵ_r) as indicated in Fig. 3(a) which shows the temperature dependence of dielectric constant of specimens as a function of sodium concentration. With the increase of sodium concentration, the ϵ_r were slightly increased up to $x=0.56$ at room temperature, and then decreased by further increasing sodium content. Two peaks of ϵ_r were observed for all of the specimens corresponding to the enlarged phase transitions from orthorhombic to tetragonal (T_{o-t}) as indicated in Fig. 3(b) and from tetragonal to cubic (T_c). The T_c and T_{o-t} did not change largely as sodium concentration increased.

Figure 4(a) shows the temperature dependence of electromechanical coupling factor (k_p) of specimen with $x=0.56$. The temperature stability of k_p was measured at an interval of 10 °C in the temperature range of -20 to 80 °C. The specimen indicated stable properties in all the temperature range, and the k_p showed a higher value of more than 0.41. Figure 4(b) shows the variations of $\Delta k_p/k_p$ 20°C and $\Delta f_r/f_r$ 20°C in the temperature range of -20 to 80 °C for specimens with $x=0.56$. The $\Delta k_p/k_p$ 20°C shows the maximum value of 0.034 at 40 °C. Also, the $\Delta f_r/f_r$ 20°C shows the maximum value of -0.025 at 50 °C.

Figure 5 shows the temperature dependence of d_{33} , g_{33} and $d_{33} \cdot g_{33}$ of specimen with $x=0.56$. The temperature stability of

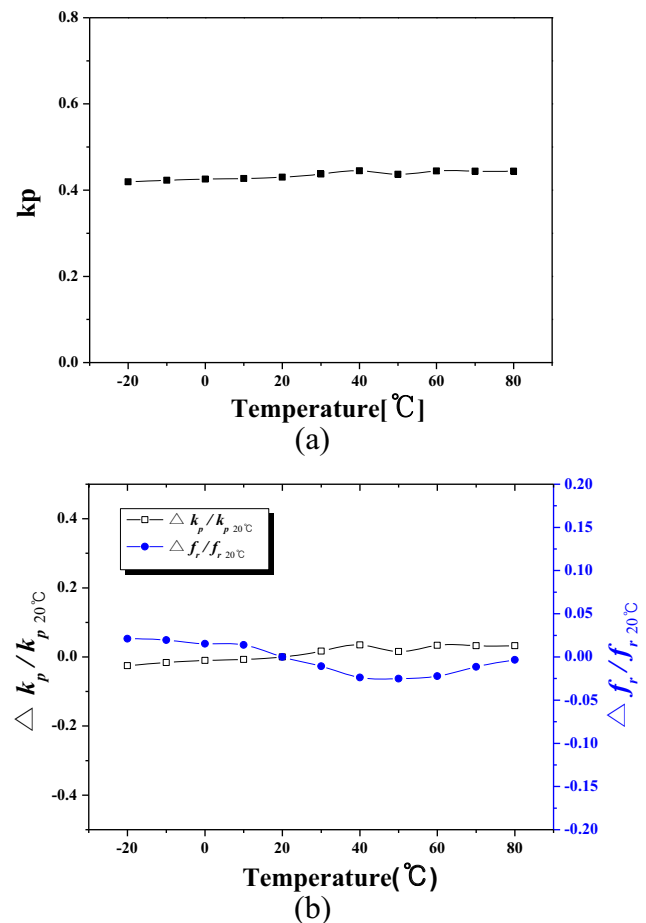


Fig. 4 Temperature dependence of electromechanical coupling factor (k_p), variations of $\Delta k_p/k_p$ 20°C and $\Delta f_r/f_r$ 20°C in the temperature range of -20 to 80 °C for $x=0.56$ specimen

them was measured at an interval of 10 °C in the temperature range of -20 to 80 °C. The $d_{33} \cdot g_{33}$ shows the maximum value of $10.72 \text{ pm}^2/\text{N}$ at 60 °C. Taking into consideration above excellent temperature stability, it is considered that the composition ceramics is suitable for the application of piezoelectric energy harvesting device in the temperature range from -20 to 80 °C.

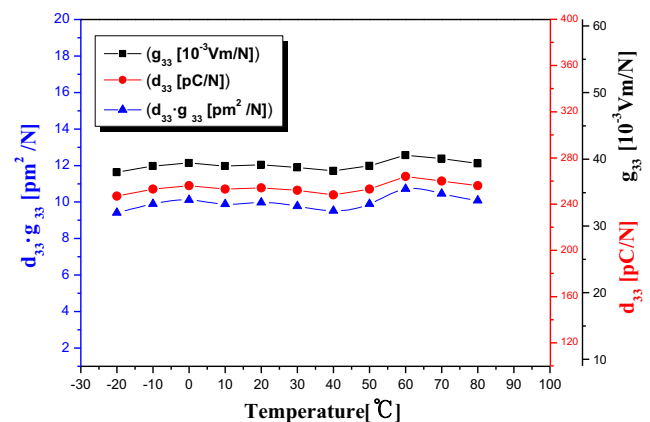


Fig. 5 Temperature dependence of variations of d_{33} , g_{33} and $d_{33} \cdot g_{33}$ in the temperature range of -20 to 80 °C for $x=0.56$ specimen

4 Conclusion

In conclusion, $N_xK_{1-x}LNTZ$ ($x=0.55\sim 0.59$) composition ceramics were fabricated using a normal sintering technique and the dielectric, piezoelectric properties and temperature stability of the ceramics were investigated. The results obtained from the experiment are as follows: The crystal structure of the entire specimen exhibited an orthorhombic phase. The $N_xK_{1-x}LNTZ$ ($x=0.56$) ceramics showed the optimum piezoelectric properties; higher physical properties of $d_{33}=261$ pC/N, $k_p=0.4366$, $\epsilon_r=735$, $\rho=4.53$ g/cm³, $d_{33}\cdot g_{33}=10.466$ pm²/N were obtained at room temperature. Also, the temperature stability of d_{33} , g_{33} and $d_{33}\cdot g_{33}$ of specimen with $x=0.56$ was an excellent. Accordingly, It is considered that the excellent temperature stability of electrical properties of specimen with $x=0.56$ is suitable for the application of piezoelectric energy harvesting device.

Acknowledgments This work was supported by Basic Science Research Program through NRF funded by the Ministry of Education, Science and Technology (No. 2010–0022117).

References

1. B. Jaffe, W.R. Cook, H. Jaffe, *Piezoelectric ceramics* (Academic Press, London, 1971), p. 135
2. J.R. Yoon, C.B. Lee, K.M. Lee, *Trans. Electri. Electro. Mater.* **11**, 126 (2010)
3. J.H. Yoo, D.H. Kim, Y.H. Lee, I.H. Lee, I.S. Kim, J.S. Song, *Integr. Ferroelectr.* **105**, 18 (2009)
4. P. Zhao, B.P. Zhang, J.F. Li, *Appl. Phys. Lett.* **90**, 242909 (2007)
5. Y. Saito, H. Takao, T. Tani, T. Nonoyama, K. Takatori, T. Homma, T. Nagaya, M. Nakamura, *Nature* **432**, 84 (2004)
6. H. Li, D. Gong, W. Yang, *J. Mater. Sci.* **48**, 1396–1400 (2013)
7. R. Zuo, J. Rödel, R. Chen, L. Li, *J. Am. Ceram. Soc.* **89**, 2010 (2006)
8. S.H. Park, C.W. Ahn, S. Nahm, J.S. Song, *Jpn. J. Appl. Phys. Part 2* **43**, L1072 (2004)
9. S.H. Lee, S.G. Lee, H.J. Kim, Y.H. Lee, *J. Electroceram.* **28**, 101–104 (2012)
10. F.R. Marcos, J.J. Romero, M.G.N. Rojero, J.F. Fernandez, *J. Eur. Ceram. Soc.* **29**, 3045–3052 (2009)
11. S. L. Ryu, S. Y. Kweon, S. C. Ur, S. C. Kim, J. H. Yoo, *J. KIEEME*, 19 (2006) 707
12. M. Matsubara, K. Kikuta, S. Hirano, *J. Appl. Phys.* **97**, 114105 (2005)
13. S. Zhang, R. Xia, T.R. Shrout, G. Zang, J. Wang, *J. Appl. Phys.* **100**, 104018 (2006)
14. K. Cho, H. Park, C. Ahn, S. Nahm, K. Uchino, S. Park, H. Lee, H. Lee, *J. Am. Ceram. Soc.* **90**, 1946 (2007)
15. H. Park, K. Cho, D. Rark, S. Nahm, H. Lee, D. Kim, *J. Appl. Phys.* **102**, 124101 (2007)
16. H.Y. Park, C.W. Ahn, H.C. Song, J.H. Lee, S. Nahm, K. Uchino, H.G. Lee, H.J. Lee, *Appl. Phys. Lett.* **89**, 062906 (2006)
17. G. Zng, J. Wang, H. Chen, W. Su, C. Wang, P. Qi, *Appl. Phys. Lett.* **88**, 212908 (2006)
18. Y.K. Oh, J.R. Noh, J.H. Yoo, J.H. Kang, L.H. Hwang, J.I. Hong, *IEEE. T. Ultrason. Ferr.* **58**, 1860 (2011)
19. Y.K. Oh, J.H. Yoo, *Mater. Lett.* **79**, 180 (2012)
20. Morozov, I. Maxim, Kungl, Hans, Hoffmann, J. Michael, *Appl. Phys. Lett.* **98**, 132908 (2011)
21. S. Zhang, J.B. Lim, H.J. Lee, T.R. Shrout, *Ferroelectrics and Frequency Control. IEEE Transactions on Ultrasonics* **56**, 1523 (2009)
22. Y. Lee, J. Yoo, K. Lee, I. Kim, J. Song, Y. Park, *J. Alloys Compd.* **506**, 872 (2010)
23. Y. Yamashita, Y. Hosono, K. Harada, N. Ichinose, *Jpn. J. Appl. Phys.* **39**, 5593 (2000)